Sterically Stabilized Anti-HER2 Immunoliposomes: Design and Targeting to Human Breast Cancer Cells *in Vitro*[†]

Dmitri Kirpotin,*[,‡] John W. Park,[§,||] Keelung Hong,[‡] Samuel Zalipsky,[⊥] Wen-Lu Li,[§] Paul Carter,[§] Christopher C. Benz,[||] and Demetrios Papahadjopoulos[‡,||]

Department of Cellular and Molecular Pharmacology, Box 0450, and Department of Hematology/Oncology, Cancer Research Institute, Box 0128, University of California, San Francisco, San Francisco, California 94143, Sequus Pharmaceuticals, Inc., 1050 Hamilton Court, Menlo Park, California 94025, and Genentech, Inc., 460 Point San Bruno Boulevard, South San Francisco, California 94080

Received August 26, 1996; Revised Manuscript Received November 4, 1996[⊗]

ABSTRACT: Liposomes (70−100 nm) of 1-palmitoyl-2-oleoylphosphatidylcholine, cholesterol, and poly(ethylene glycol) (PEG)-modified phosphatidylethanolamine (PEG-DSPE) were conjugated to Fab′ fragments of a humanized recombinant MAb against the extracellular domain of HER2/*neu* to create sterically stabilized immunoliposomes (anti-HER2 SL) as a drug carrier targeting HER2-overexpressing cancers. Conjugation employed maleimide-terminated membrane-anchored spacers of two kinds: a short spacer, providing attachment of Fab′ close to the liposome bilayer, or a long spacer, with Fab′ attachment at the distal terminus of the PEG chain. Confocal microscopy and spectrofluorometry of HER2-overexpressing breast cancer cells incubated with fluorescently labeled anti-HER2 SL prepared with either spacer showed binding of liposomes (8000−23 000 vesicles/cell) followed by endocytosis (rate constant k_e = 0.012−0.033 min^{-1}) via the coated-pit pathway, evidenced by intracellular acidification and colocalization with transferrin. Uptake of anti-HER2 immunoliposomes by breast cancer cells with low HER2 expression, or after preincubation of cells with free anti-HER2 Fab′, was less than 0.2% and 4.3%, respectively, of the uptake by HER2-overexpressing cells. Increasing PEG-DSPE content (up to 5.7 mol %) in anti-HER2-SL prepared with the short spacer decreased liposome−cell binding affinity 60−100-fold, while k_e decreased only 2-fold; however, when Fab′ fragments were conjugated via a PEG spacer, both binding afffinity and k_e were unaffected by PEG-DSPE content. Cell binding and internalization of anti-HER2 immunoliposomes increased at higher surface density of conjugated Fab′ fragments, reaching plateaus at ∼40 Fab′/liposome for binding and ∼10−15 Fab′/liposome for internalization. Uptake of anti-HER2 immunoliposomes correlated with the cell surface density of HER2 and significantly ($p < 0.005$) correlated with the antiproliferative effect of the targeting antibody but not with the total level of cellular HER2 expression. The results obtained were used to optimize *in vivo* preclinical studies of anti-HER2 SL loaded with antineoplastic drugs.

Antibody-based targeting is a promising approach in the development of targeted therapies for cancer (Begent, 1990; Bator & Reading, 1991). Among various antigens found on malignant cells, glycoprotein p185^{HER2}, a member of the EGFR[1] family of receptor tyrosine kinases encoded by the HER2/*neu* (c-erbB-2) protooncogene, is an attractive target for therapy. This protein is overexpressed in various cancers, including breast, lung, and ovarian carcinomas (Slamon *et al.*, 1989; Tripathy & Benz, 1992; De Potter, 1994; Molland *et al.*, 1996). Overexpression of p185^{HER2} is also unique to the malignant phenotype (Press *et al.*, 1990). A variety of p185^{HER2}-specific monoclonal antibodies have been developed (Tagliabue *et al.*, 1989; Hudziak *et al.*, 1991) and used for the delivery of conjugated toxins (Rodriguez *et al.*, 1993; Wels *et al.*, 1995), prodrug activators (Eccles *et al.*, 1994; Rodrigues *et al.*, 1995), cytotoxic lymphocyte recognition markers (Shalaby *et al.*, 1995; Wels *et al.*, 1995; Zhu *et al.*, 1995), and plasmid DNA (Fominaya & Wels, 1996) to HER2-overexpressing tumor cells in culture and in animal models.

4D5, a murine MAb directed against the extracellular domain of p185^{HER2}, binds to abundant sites on the surface of HER2-overexpressing cells and elicits a partially agonistic response, which includes receptor internalization and phosphorylation, and ultimately yields inhibition of cell prolifera-

[†] This work was supported by NIH Grant P50CA58207.

* Address correspondence to this author. Telephone: (415) 476-4828. Fax (415) 476-0688. E-mail: dkizpo@itsa.ucsf.edu.

[‡] Department of Cellular and Molecular Pharmacology, University of California, San Francisco.

[§] Genentech, Inc.

[||] Department of Hematology/Oncology, University of California, San Francisco.

[⊥] Sequus Pharmaceuticals, Inc.

[⊗] Abstract published in *Advance ACS Abstracts,* December 15, 1996.

[1] Abbreviations: Chol, cholesterol; DSPE, 1,2-distearoyl-3-*sn*-glycerophosphoethanolamine; EDTA, ethylenediaminetetraacetic acid; EGF, epidermal growth factor; EGFR, EGF receptor; HEPES, *N*-(2-hydroxyethyl)piperazine-*N*′-2-ethanesulfonic acid; HBS, HEPES-buffered saline (20 mM HEPES-Na, 144 mM NaCl, pH 7.2); HPTS, 8-hydroxypyrenetrisulfonic acid trisodium salt; MMC, 4-(*N*-maleimidomethyl)cyclohexane-1-carboxylate; MP, β-(*N*-maleimido)propionyl; MP-PEG-SC, ω-MP-amidopoly(oxyethylene)-α-succinimidyl carboxylate; PBS, phosphate-buffered saline (KH_2PO_4, 0.2 g/L; Na_2HPO_4·$7H_2O$, 2.16 g/L; KCl, 0.2 g/L; NaCl, 8.0 g/L; pH 7.4); PE, phosphatidylethanolamine; PEG, poly(ethylene glycol); PEG-DSPE, *N*-[ω-methoxypoly(oxyethylene)-α-carbonyl]-DSPE; POPC, 1-palmitoyl-2-oleoyl-3-*sn*-glycerophosphocholine; Rho-PE, *N*-(lissamine rhodamine B sulfonyl)phosphatidylethanolamine; rhuMAbHER2, recombinant humanized anti-p185^{HER2} monoclonal antibody; SL, sterically stabilized liposomes.

S0006-2960(96)02148-4 CCC: $14.00

tion (Hudziak *et al.*, 1989). A recombinant, fully humanized version of 4D5 (rhuMAbHER2) has antiproliferative activity against HER2-overexpressing cancers *in vitro* and *in vivo* (Carter *et al.*, 1992). We have recently described a liposomal drug delivery system targeted to HER2-overexpressing cancer cells by attachment of Fab′ fragments of rhuMAb-HER2 to the membrane of small unilamellar liposomes using an amphiphilic maleimide-terminated anchor MMC-PE (Park *et al.*, 1995). Such anti-HER2 immunoliposomes bind to the cell surface and become avidly endocytosed by the target cells. Loading of anti-HER2 immunoliposomes with doxorubicin provides superior toxicity against HER2-overexpressing breast cancer cells, in comparison to nontargeted liposomal doxorubicin, while causing minimal toxicity against nonmalignant cells *in vitro*.

Liposomal anticancer pharmaceuticals benefit from "steric stabilization" achieved by conjugation of poly(ethylene glycol) to the liposome surface (Woodle & Lasic, 1992; Lasic & Papahadjopoulos, 1995). Sterically stabilized liposomes have lower reticuloendothelial uptake, prolonged circulation time in the blood, and higher accumulation in tumors (Papahadjopoulos *et al.*, 1991; Papahadjopoulos & Gabizon, 1995). However, our previous study showed that surface-grafted PEG (M_r 2000) at more than 1.3 mol % of total lipid (2% of total phospholipid) substantially reduced the uptake and cytotoxicity of doxorubicin-loaded anti-HER2 immunoliposomes in the cultures of target cells (Park *et al.*, 1995).

In the present work, we explore the hypothesis that the mode of anti-p185^{HER2} Fab′ conjugation to the liposome in relationship to membrane-anchored amphipathic PEG affects the functional interaction between the anti-HER2 immunoliposome and the target cell. We analyze the process of Fab′−immunoliposome binding and internalization into HER2-overexpressing target cells, with regard to Fab′ density and level of HER2 overexpression. On the basis of these studies, we offer a new, modified design of sterically stabilized anti-HER2 immunoliposomes that exhibit high levels of selective internalization by HER2-overexpressing breast cancer cells.

MATERIALS AND METHODS

Materials

Phospholipids and *N*-(lissamine rhodamine B sulfonyl)-phosphatidylethanolamine (egg transphosphatidylated) were obtained from Avanti Polar Lipids (Alabaster, AL); cholesterol was obtained from Calbiochem (San Diego, CA); 8-hydroxypyrenetrisulfonic acid trisodium salt was obtained from Molecular Probes (Eugene, OR). MMC-DSPE was synthesized from *N*-succinimidyl-4-(*N*′-maleimidomethyl)-cyclohexane-1-carboxylate (Sigma, St. Louis, MO) and DSPE according to Martin and Papahadjopoulos (1982). *ω*-*N*-(*β*-Maleimidopropionyl)aminopoly(oxyethylene)-α-*N*-succinimidyl carbonate derived from PEG with M_r 2000 was from Shearwater Polymers (Huntville, AL); organic solvents (HPLC grade) and silica-60 TLC plates were from Fisher (Pittburgh, PA); other chemicals were of reagent purity from Sigma (St. Louis, Mo). Methoxy-PEG-DSPE and amino-PEG-DSPE were prepared from PEG (M_r 1900) according to Zalipsky (1993) and Zalipsky *et al.* (1994). Fab′ fragments of rhuMAbHER2 were prepared as described (Park *et al.*, 1995). Cell lines were obtained and cultured as previously described (Lewis *et al.*, 1993; Scott *et al.*, 1993; Park *et al.*, 1995). Media were supplied by the UCSF Cell Culture Facility.

Methods

Synthesis of Maleimido-PEG-DSPE. Poly(ethylene glycol) derivatives of phosphatidylethanolamine modified with a maleimide group at the distal terminus of the poly(ethylene glycol) chain were synthesized by two methods (Figure 1). In the first method, amino-PEG-DSPE (Zalipsky *et al.*, 1994) (500 mg, 0.18 mmol) and *N*-succinimidyl-3-(*N*-maleimido)-propionate (62.6 mg, 24 mmol) were dissolved in CH_2Cl_2 (3 mL) and DMF (0.75 μL) followed by triethylamine (76 μL, 0.54 mmol). After 15 min TLC ($CHCl_3$:CH_3OH:H_2O = 90:18:2, visualized with ninhydrin spray) showed that the reaction was complete. The product mixture was purified on the silica gel column eluted with a stepwise gradient of methanol (0−14%) in chloroform. The pure product-containing fractions (eluted in $CHCl_3$:CH_3OH = 88:12) were combined and evaporated and then further dried in vacuo over P_2O_5, yielding MP-PEG-DSPE as a white solid (202.8 mg, 44.2%). ^{1}H NMR (CD_3OD): δ 0.88 (multiplet, 6H), 1.26 (s, CH_2, 56H), 1.58 (br m, CH_2CH_2C═O, 4H), 2.31 (2 t, CH_2C═O, 4H), 2.48 (t, MP-CH_2CH_2C═O), 3.53 (t, CH_2N, 2H), 3.63 (s, PEG, 180H), 3.88 and 3.98 (q and t, CH_2PO_4-CH_2, 4H), 4.20 (t, CH_2O_2CN, 2H), 4.17 and 4.39 (2 dd, OCH_2CHCH_2OP, 2H), 5.2 (m, $PO_4CH_2CHCH_2O$, 1H), 6.69 (s, maleimide, 4H). In the similar way, MMC-PEG-DSPE was prepared from *N*-succinimidyl 4-(*N*′-maleimidomethyl)-cyclohexane-1-carboxylate with 70% yield (DSPE). In the second method, MP-PEG-SC (100 mg, 50 μmol) was reacted with DSPE (35 mg, 46 μmol) and triethylamine (13.6 μL, 100 μmol) in 2 mL of chloroform for 4 h at 45 °C. The product was purified by chromatography on silica gel as above and obtained with the yield of 74% (DSPE). All products revealed single spots on TLC (silica 60; $CHCl_3$:MeOH:H_2O = 65:25:4) after visualization by iodine vapor and molybdate spray. After solubilization of the products in the presence of 1% Triton X-100, maleimide groups were assayed according to Sedlack and Lindsay (1968); phosphate groups were quantified according to Morrison (1964). The ratio of maleimide to phosphate groups was found to be 0.90−1.0 (theory, 1.0).

Liposome Preparation. Liposomes were prepared from POPC and Chol (3:2 molar ratio) by lipid film hydration, followed by membrane extrusion (Olson *et al.*, 1979). When indicated, mPEG-DSPE was included into the lipid mixture at an amount of 0.6−5.7 mol % of total lipid. For antibody conjugation, the maleimide-terminated phospholipid derivative was included at 1.2 mol % of total lipid. When maleimido-PEG-DSPE was used as a linker, PEG-DSPE content was calculated as the total of maleimide-terminated and methoxy-terminated PEG-DSPE. For confocal microscopy studies, 0.1 mol % of fluorescently labeled phospholipid (Rho-PE) was added to the lipid mixture. Multilamellar liposomes formed by shaking of the dry lipid film in HBS or in solution containing 35 mM HPTS, pH 7.0, adjusted to an osmolarity of 280 mOsm/L with NaCl, were extruded 10 times at room temperature through two stacked 0.1 μm polycarbonate membranes. When appropriate, unentrapped HPTS was removed by gel filtration on Sephadex G-25, and the liposomes were stored at approximately 5 mM phospholipid in HEPES-buffered saline at 4 °C. Liposome size was measured by dynamic laser light scattering (Coulter N4 particle size analyzer); liposome concentration was deter-

mined by phospholipid phosphate assay (Morrison, 1964) and expressed as molar concentration of liposome phospholipid.

Conjugation of Anti-HER2 Fab′ to Liposomes. Fab′ fragments of rhuMAbHER2 were added to the liposomes (7−10 mM) containing maleimide-terminated linker in HEPES-buffered saline at the ratio of 0.3 mg of protein/mL, and after pH adjustment to 7.3−7.4 (NaOH) the mixture was incubated overnight at ambient temperature under argon. Excess maleimide groups were quenched by incubation with 2 mM β-mercaptoethanol for 30 min; β-mercaptoethanol and unconjugated antibody were removed by gel chromatography on Sepharose 4B (eluant HBS). Immunoliposomes were collected in the void volume fraction, sterilized by passage through a 0.2 μm sterile filter, and stored at 4 °C. The amount of conjugated Fab′ in the immunoliposomes was determined by dye binding assay (Bio-Rad) and converted into the number of Fab′ per liposome, assuming a liposome size of 100 nm, an average area per phospholipid molecule of 75 Å^2, which gives 80 000 phospholipid molecules/vesicle (Marsh, 1990), and a molecular weight of the rhuMAbHER2 Fab′ fragment equal to 46 000. To prepare immunoliposomes with various amounts of conjugated antibody, the initial ratio of Fab′ to maleimide-activated liposomes was varied.

Confocal Microscopy of the Cellular Uptake of Anti-HER2 Immunoliposomes. SK-BR-3 and MCF-7 cells were grown on coverslips to subconfluency. Cells were coincubated with Rho-PE-labeled anti-HER2 SL and FITC-labeled transferrin at saturating concentrations in serum-supplemented growth media at 37 °C for varying time periods, washed extensively with PBS, mounted in glycerol, and observed with a Molecular Dynamics MultiProbe 2001 confocal microscope.

Spectrofluorometric Measurement of Immunoliposome Uptake by the Cells. Simultaneous quantitation of cell surface-bound and endocytosed liposomes was performed according to Straubinger *et al.* (1990). Cells grown to subconfluency were incubated at 37 or 4 °C with HPTS-loaded anti-HER2 immunoliposomes diluted to 0.025 mM phospholipid in 10% serum-supplemented growth medium. For comparison of the liposome uptake by cells with different HER2 expression, the cells were incubated for 2 h with 0.1 mM anti-HER2 immunoliposomes in the growth media at 37 °C. The cells were then rinsed four times with ice-cold HEPES-buffered saline and harvested in 5 mM EDTA/PBS, and the fluorescence excitation spectra of the cell suspensions in the range of 400−500 nm were recorded using a SPEX Fluorolog 2 photon counting spectrofluorometer (SPEX Industries, Edison, NJ) at an emission wavelength of 512 nm. After subtraction of autofluorescence, the fluorescence intensities at excitation wavelengths of 454 nm (I_{454}) and 413 nm (I_{413}) were determined. The total amount of cell-associated liposomes ("liposome uptake") was determined from I_{413} by comparison to the fluorescence of liposome standards. The proportion of liposomes bound to the cell surface (neutral pH compartment) ($[L]_s$) was found from the formula:

$$\%\,[L]_s = (r - r_0)/(r_{100} - r_0) \times 100 \qquad (1)$$

where $r = I_{454}/I_{413}$ of the sample, $r_{100} = I_{454}/I_{413}$ of the liposomes in the cell harvesting buffer (pH 7.4), and $r_0 = I_{454}/I_{413}$ of the endocytosed liposomes. The latter ratio was determined from the fluorescent spectra of cells incubated with HPTS-loaded anti-HER2 immunoliposomes for 2 h and postincubated in the liposome-free medium for 3 h, which afforded complete endocytosis of the cell-associated liposomes (Park *et al*., 1995). The amounts of cell surface-bound and endocytosed liposomes, normalized to the cell concentrations, were plotted vs incubation time, and the kinetic curves obtained were used to characterize the uptake of liposomes by the cells. Internalization of the liposomes was characterized by the first-order endocytosis rate constant (k_e) derived from the above kinetic curves using the formula (Lee *et al.,* 1993):

$$k_e = (d[L]_i/dt)_{ss}/[L]_{s,ss} \qquad (2)$$

where $[L]_i$ is the amount of internalized liposomes (per unit cell concentration), $[L]_s$ is the amount of cell surface-bound liposomes, $(d[L]_i/dt)_{ss}$ is the liposome uptake rate at the steady state determined as the slope of the curve $[L]_i$ vs time at the steady-state time point ($d[L]_s/dt = 0$), and $[L]_{s,ss}$ is the steady-state concentration of cell surface-bound liposomes. To assess the effect of free antibody on the liposome−cell interactions, free Fab′ fragments of rhuMabHER2 were added to the cells 30 min prior to addition of the liposomes.

Immunoliposome Binding to SK-BR-3 Cells. The plated cells were incubated with serial dilutions of HPTS-loaded immunoliposomes (0.2−500 μM of liposomal phospholipid) in the cell growth medium for 7 h under gentle agitation. To avoid endocytosis of the bound liposomes, the incubation was carried out at 4 °C. After incubation, the cells were washed and harvested, and the amount of cell-associated liposomes was determined by fluorometry as described above. The dissociation constant of the liposome−cell complex (K_{diss}) and the maximum liposome−cell binding ($[L]_{s,max}$) were determined as best fit parameters of the equation:

$$[L]_s = [L]_{s,max}[L]_0/(K_{diss} + [L]_0) \qquad (3)$$

where $[L]_s$ is the amount of cell-bound liposomes per 10^6 cells and $[L]_0$ is the concentration of liposomes in the incubation medium. Since the amount of cell-associated liposomes was always less than 2% of the total, the concentration of free liposomes in the incubation medium at equilibrium was assumed to be equal to the initial liposome concentration, and the applicability of eq 3 was warranted. Best fit parameters were calculated using Sigma Plot 4.1 software (Jandel Scientific, Corte Madera, CA).

Statistical Methods. All experimental points are the mean of at least three parallel runs; unless indicated otherwise, standard errors were less than 8%. Standard errors for binding and kinetic parameters, as well as correlation coefficients for linear regressions, were obtained as part of computational routines used by Sigma Plot 4.1. Probabilities of null hypothesis for correlation were calculated using Student's *t*-test.

RESULTS

We have used two types of membrane-bound maleimide-terminated linkers for the conjugation of anti-HER2 Fab′ fragments to liposomes utilizing the unique free thiol group in the Fab′ hinge region. In the first type, a linker with a short spacer group, MMC-DSPE, provided attachment of the antibody fragments close to the liposome bilayer (Martin &

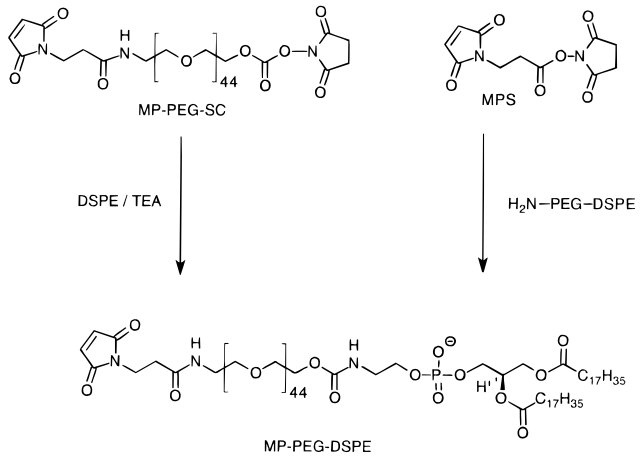

FIGURE 1: Synthesis of PEG-DSPE derivatives with the maleimide function at the end of the poly(ethylene glycol) chain.

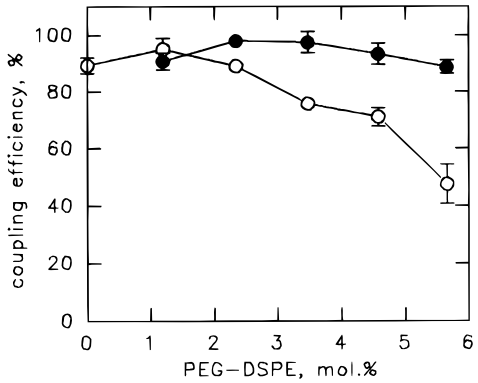

FIGURE 2: Coupling efficiency of Fab′ to maleimide-activated SL with various amounts of PEG-PE. Conjugation linker: MMC-PE (short spacer) (○); MP-PEG (M_r 2000)-DSPE (long spacer) (●). Coupling efficiency: amount of liposome-conjugated protein as percent of total protein taken for conjugation.

Papahadjopoulos, 1982). The use of the *N*-(maleimidomethyl)cyclohexyl group allowed practically quantitative conjugation of anti-HER2 to the liposomes, limited only by the proportion of reduced thiol groups in the antibody preparation. However, surface-grafted PEG chains (M_r = 2000) were likely to disturb the interaction between conjugated Fab′ and its target antigen (Klibanov *et al*., 1990; Park *et al*., 1995). Therefore, in the second approach, Fab′ were conjugated to the termini of PEG chains. For this approach, we synthesized two linkers, MMC-PEG-DSPE and MP-PEG-DSPE, bearing maleimide groups at the distal end of the PEG chain attached to a hydrophobic membrane anchor DSPE. Two methods were used (Figure 1): coupling of *N*-succinimidyl maleimidopropionate to the amino group of H_2N-PEG-DSPE prepared as described earlier (Zalipsky *et al*., 1994) or coupling of DSPE to a heterobifunctional PEG derivative, MP-PEG-SC, constructed in analogy to similar SC derivatives of the polymer (Zalipsky, 1993; Zalipsky *et al*., 1994; Allen *et al*., 1995). Both methods were equally effective and resulted in comparable yields of the maleimido-PEG-DSPE. MMC derivatives were formed by the first method using the *N*-hydroxysuccinimidyl ester of 4-(*N*′-maleimidomethyl)cyclohexanecarboxylic acid. Both MP and MMC end-group functionalized PEG-DSPE derivatives proved equally effective for preparation of immunoliposomes. In the liposomes containing up to 2.3 mol % of PEG-DSPE, maleimido-PEG-DSPE derivatives provided conjugation with the same efficiency as their counterparts without the long PEG spacer (Figure 2); however, when the content of PEG-DSPE increased to 3.5 mol % and more, which corresponds to the transition from "mushroom" to "brush" conformation of the liposome-grafted PEG (Kenworthy *et al*., 1995b), the conjugation efficiency of the short-chain maleimide linker decreased, while in the case of PEG-spacer linkers, the conjugation was practically quantitative up to the maximum PEG-DSPE content studied (5.7 mol %) (Figure 2). At the chosen protein/lipid ratio, the conjugation resulted in 60−80 Fab′/liposome, while by increasing the Fab′/lipid ratio in the conjugation mixture this number could be increased to 100−120 Fab′/liposome without any loss in the coupling efficiency. HPTS-loaded liposomes released less than 1% of entrapped solute during Fab′ conjugation and subsequent incubation at 37 °C in the presence of 10% serum. Immunoliposomes were stored for several months at 4 °C in the HBS buffer without any detectable leakage of entrapped HPTS or reduction in uptake by HER2-overexpressing cells.

Confocal fluorescence microscopy studies were performed to visualize the internalization and subsequent intracellular distribution of immunoliposomes. Immunoliposomes containing 3.82 mol % of PEG-DSPE, conjugated to anti-HER2 Fab′ via the MMC-PEG-DSPE derivative and labeled with Rho-PE, were incubated with SK-BR-3 breast cancer cells, which overexpress HER2 (10^6 molecules/cell), and with MCF-7 breast cancer cells which have very low or basal levels of HER2 expression (10^4 receptors/cell) (Lewis *et al.*, 1993). As an additional control, cells were coincubated with FITC-labeled transferrin, a ligand which undergoes rapid receptor-mediated endocytosis (Vidal *et al.*, 1987) in both cell lines. After 10 min incubation immunoliposomes remained largely at or near the cell surface accompanied by some cytoplasmic localization (Figure 3A), compared with the rapid endocytosis of transferrin (Figure 3A). By 30 min, immunoliposomes were observed distributed throughout the cytoplasm and extensively colocalized with transferrin in endocytic vesicles as evident from superimposed images of rhodamine and fluorescein fluorescence (Figure 3B). The specificity of immunoliposome uptake was confirmed by preincubation of SK-BR-3 cells with rhuMAbHER2 at 10-fold excess over immunoliposomes; preincubation was able to block immunoliposome uptake but not that of transferrin. In addition, MCF-7 cells similarly incubated with immunoliposomes and transferrin showed uptake of transferrin but no detectable uptake of immunoliposomes (Figure 3C).

To quantitate the cellular uptake, the liposomes were prepared with encapsulated pH-sensitive, membrane-impermeable fluorescent marker (HPTS). Entry of HPTS-loaded liposomes into the acidic environment of endocytic vesicles causes a sharp decrease in fluorescence at λ_{ex} 454 nm while its fluorescence at the isosbestic point (λ_{ex} 413 nm) remains unchanged, therefore allowing simultaneous quantitation of total vs endosome-localized cell-associated liposomes (Straubinger *et al.*, 1990). Upon incubation of HPTS-loaded anti-HER2 immunoliposomes with SK-BR-3 cells, we observed a progressive decrease in the I_{454}/I_{413} fluorescence ratio, indicating the transfer of cell-associated liposomes from the neutral to low pH compartment (Figure 4). As a control, subsequent incubation with a lysosomotropic agent (NH_4-Cl) was performed and, as expected, resulted in an increase of pH in the cellular compartments harboring anti-HER2 immunoliposomes. This effect could be reversed by removal

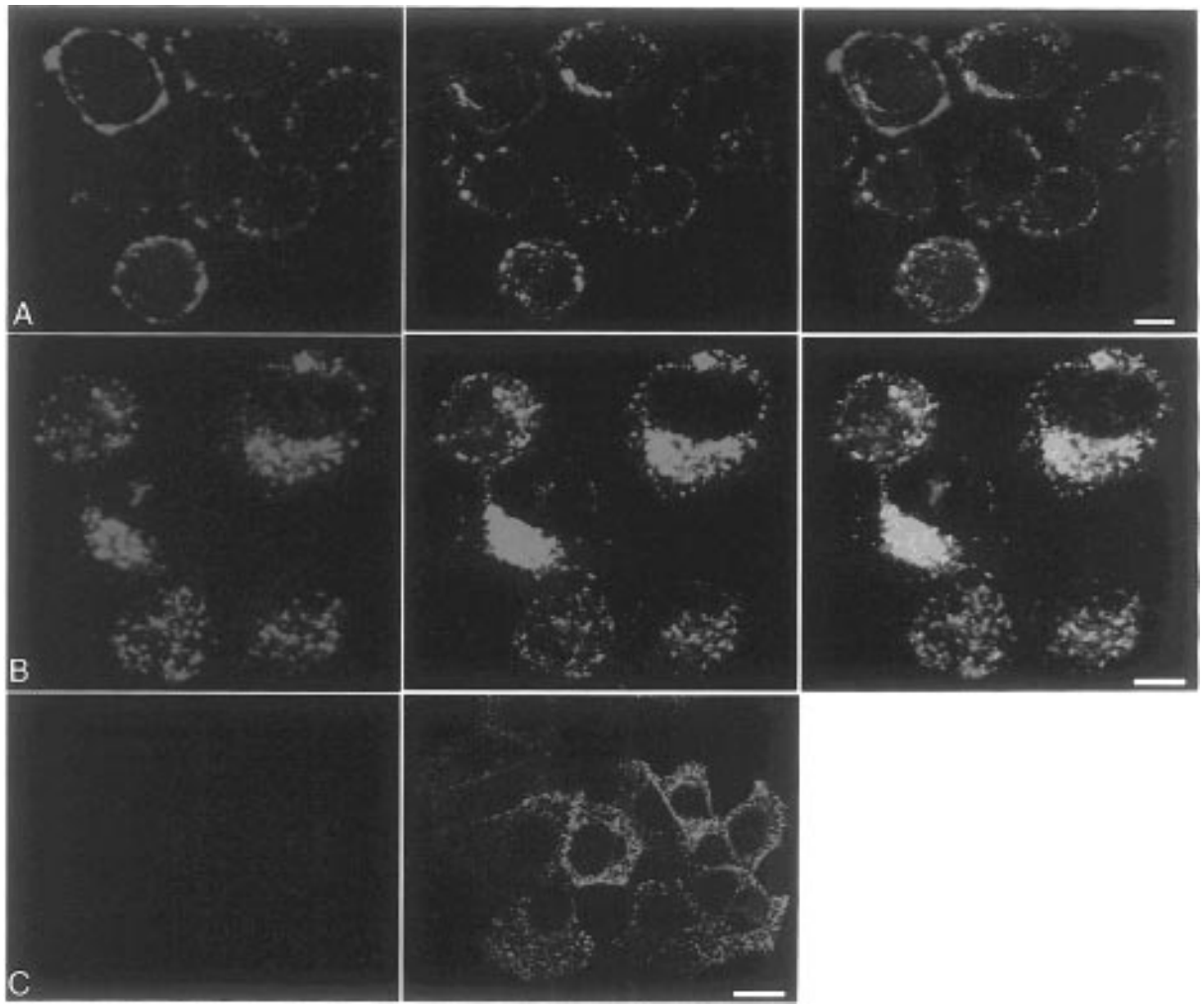

FIGURE 3: Confocal microscopy of cells coincubated at 37 °C with rhodamine-labeled anti-HER2 immunoliposomes (3.5 mol % PEG-DSPE, Fab′ conjugated via PEG spacer) and fluorescein-labeled transferrin: left column, liposomes (red); central column, transferrin (green); right column, superimposed images. SK-BR-3 cells: incubation time 10 min (A) and 30 min (B). MCF-7 cells: incubation time 30 min (C). Scale bar 10 = μm.

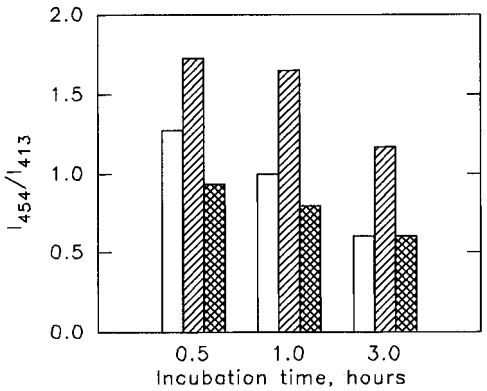

FIGURE 4: Ratio of HPTS fluorescence at excitation wavelengths 454 and 413 nm (I_{454}/I_{413}) after incubation of HPTS-loaded anti-HER2 immunoliposomes with SK-BR-3 cells (100 μM liposome phospholipid in cell growth medium at 37 °C). At indicated times, cells were washed with PBS and treated with 5 mM NH_4Cl in PBS for 20 min. Bars: open, cells before treatment with NH_4Cl; dashed, cells after NH_4Cl treatment; cross-hatched, cells after removal of NH_4Cl and 20 min postincubation in fresh medium.

of NH_4Cl (Figure 4). These data indicated that cell-associated liposomes were indeed localized in endosomes and lysosomes. A 30-min preincubation of SK-BR-3 cells with free rhuMAbHER2 Fab′ at 10-fold molar concentration relative to liposome-conjugated Fab′ reduced the uptake of anti-HER2 immunoliposomes (25 μM phospholipid) to 4.3% of its value without free Fab′. Finally, the cellular uptake of SL without conjugated anti-HER2 Fab′ (but with the thiol-quenched maleimide-terminated linker) even after prolonged incubation at the highest studied concentration (1 mM) was less than 0.01 nmol/10^6 cells, or less than 1% of the uptake of anti-HER2 immunoliposomes (Table 3).

To assess the effect of Fab′ density on immunoliposome uptake by target cells, HPTS-loaded anti-HER2 immunoliposomes containing a range of 6−81 Fab′/liposome were incubated with SK-BR-3 cells for 2−6 h. The amount of total cell-associated immunoliposomes increased with increasing density of liposome-conjugated anti-HER2 Fab′ until the plateau was reached at about 40 Fab′/liposome, or one Fab′ per 1000 phospholipid molecules in the outer leaflet of the liposome bilayer (Figure 5A). This result suggested that there is no need to increase the amount of liposome-conjugated protein over 40 Fab′/vesicle in order to achieve efficient delivery of anti-HER2 immunoliposomes into target (HER2-overexpressing) cells. An even lower number of liposome-conjugated Fab′ fragments was required to ensure internalization of the surface-bound anti-HER2 immunoliposomes. Already at the lowest Fab′ density studied (~6 Fab′/liposome, or one Fab′ per 8000 phospholipids in the outer leaflet) 55−60% of the cell-associated anti-HER2 immunoliposomes were endocytosed, and this value reached 80−95% for the liposomes bearing more than 10−15 Fab′/

Table 1: Uptake of Anti-HER2 Immunoliposomes by Cancer Cells with Various Levels of $p185^{HER2}$ Expression

cell line[a]	total uptake, nmol of PL/mg of cell protein	% endocytosed	$p185^{HER2}$ expression[b] total[c]	$p185^{HER2}$ expression[b] surface[d]	cell proliferation, anti-HER2 muMAb (4D5) treated vs untreated cells,[b] %
SK-BR-3	7.21 ± 0.45[e]	88 ± 1.4	917	33.0	33
MDA-MB-453	6.52 ± 0.22	80.8 ± 0.7	43.7	16.7	61
BT-474	4.47 ± 0.21	90.4 ± 1.1	548	25.0	27
MCF-7	<0.01	0	7.27	1.2	101
MCF-7−18	4.25 ± 0.17	66.2 ± 1.9	NA	NA	NA
SK-OV-3	0.837 ± 0.096	72 ± 2.7	537	16.7	77
MKN-7	0.236 ± 0.021	13.4 ± 7.3	194	16.7	99

[a] Cells: SK-BR-3, BT-474, MDA-MB-453, MCF-7, breast carcinomas; MCF-7−18, MCF-7 stably transfected with HER2/*neu*; SK-OV-3, ovarian carcinoma; MKN-7, gastric carcinoma. [b] From Lewis *et al.* (1993). [c] ng/mg of cell protein. NA, data not available. [d] Flow cytometry using muMAb (4D5) as a marker; relative to normal mammary epithelial cells (line 184). [e] Mean ± SE.

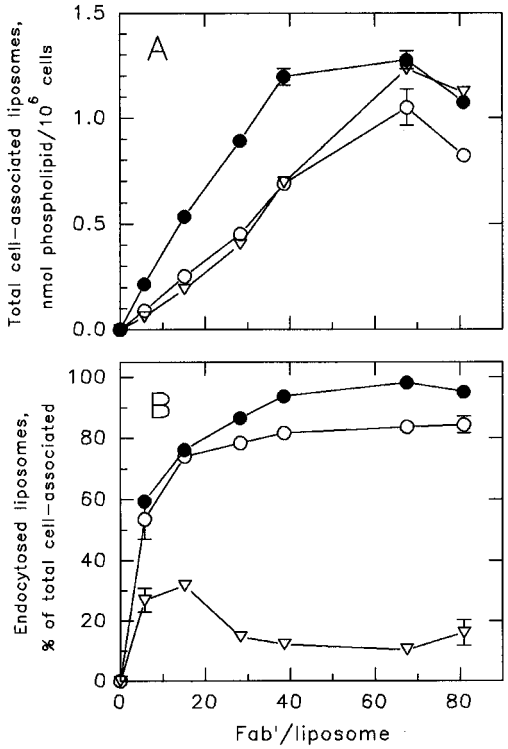

FIGURE 5: Effect of the density of liposome-conjugated anti-HER2 Fab′ on the total uptake and internalization of anti-HER2 immunoliposomes by SK-BR-3 cells: (A) total uptake; (B) endocytosed liposomes as percent of total uptake. Incubation: 2 h at 37 °C (○); 6 h at 37 °C (●); 2 h at 4 °C (▽). Liposome concentration: 25 μM of liposome phospholipid.

vesicle (Figure 5B), suggesting that liposome binding to the cells was the factor determining the extent of liposome uptake. Indeed, when the incubation was carried out at 4 °C, the total amount of cell-associated liposomes did not differ significantly from that at 37 °C, while the fraction of endocytosed liposomes was greatly reduced (Figure 5A).

Breast carcinomas, as well as other cancers, display a variety of HER2 expression levels ranging from less than10^4 to 10^6 molecules/cell. In order to develop criteria for the future clinical use of HER2-targeted liposomal pharmaceuticals, it was of interest to study the effect of HER2 expression level on the uptake of anti-HER2 immunoliposomes. Table 1 shows the uptake (i.e., total cell-associated amount), as well as the percent of endocytosed anti-HER2 immunoliposomes (81 Fab′/vesicle; no PEG-DSPE) by cell lines expressing different levels of HER2. All four HER2-overexpressing breast cancer cell lines showed high uptake of anti-HER2 immunoliposomes, while the uptake by the cells that do not overexpress HER2 (MCF-7) was less than 1% of the value characteristic for HER2-positive cells. Two cell lines, MKN-7 (gastric carcinoma) and SKOV-3 (ovarian carcinoma), showed lower than expected uptake of anti-HER2 immunoliposomes despite high levels of HER2 expression (Lewis *et al.*, 1993). The differences in cellular uptake of immunoliposomes between these HER2-overexpressing lines could not be explained by the release of soluble extracellular domain of $p185^{HER2}$ (which would block the antigen binding sites of liposome-conjugated Fab′) since the uptake was identical in fresh or conditioned (3 days) growth medium. We suggested that the cellular uptake of anti-HER2 immunoliposomes may be determined not only by the cellular abundance of their target antigen, HER2 protein, but also by its functional activation as a result of such binding. MKN-7, a highly HER2-positive cell line, presented an interesting case to illustrate this point. Apart from the full-length $p185^{HER2}$, MKN-7 cells express also a truncated version or this protein, which consists essentially of its extracellular domain, as a result of alternative splicing (Scott *et al.*, 1993). The truncated HER2 protein still provides a binding site for an anti-HER2 antibody or immunoliposome but would not functionally respond to such binding by internalization and, eventually, antiproliferative effect (Lewis *et al.*, 1993). Also, the lack of the full-size membrane-spanning domain would make the complex between immunoliposome and truncated HER2 prone to dissociation from the membrane, resulting in the even lower uptake. Indeed, the uptake of anti-HER2 immunoliposomes did not show a statistically significant correlation with the total amount of cellular $p185^{HER2}$ recognizable by the target antibody but correlated better with the density of cell-surface expressed $p185^{HER2}$, and a statistically significant ($p < 0.005$) correlation was observed between the uptake of immunoliposomes and the antiproliferative activity of anti-HER2 MAb 4D5, a murine prototype of the humanized recombinant MAb used in this study (Table 2). This finding supports the hypothesis that the uptake of anti-HER2 immunoliposomes is likely to be determined not only by the density of HER2 protein but also by the ability of this protein to become functionally activated as a result of interaction with the immunoliposome.

Surface-attached PEG has been shown to interfere with the association of targeted liposomes to their cellular and molecular targets (Klibanov *et al.*, 1990; Park *et al.*, 1995). Such interference may be circumvented by conjugation of the antibody to the distal end of the PEG chains attached to the liposome surface (Hansen *et al.*, 1995; Zalipsky *et al.*, 1996). Indeed, when the short linker MMC-PE was used for preparation of anti-HER2 SL (65−90 Fab′/vesicle), inclusion of 5.7 mol % of PEG-DSPE into the liposome composition reduced their uptake (i.e., total of binding and endocytosis) by SK-BR-3 cells by an order of magnitude,

Table 2: Correlation Coefficients and Probabilities of Null Hypothesis (p) for Linear Correlation between the Uptake of Anti-HER2 Immunoliposomes, Cellular HER2 Expression, and Responsiveness of Target Cells to Anti-HER2 Antibody

uptake/parameter	total cellular p185^{HER2}	cell surface p185^{HER2}	antiproliferative effect of anti-p185^{HER2} MAb (4D5)
total	0.434 ($p = 0.398$)	0.724 ($p = 0.112$)	0.835 ($p = 0.0040$)
internalized only	0.477 ($p = 0.380$)	0.744 ($p = 0.089$)	0.863 ($p = 0.0028$)

Table 3: Binding and Internalization Parameters of Anti-HER2 Immunoliposomes with Various PEG-DSPE Content by SK-BR-3 Cells

PEG-DSPE, mol % of total lipid	conjugation spacer	Fab′/vesicle	K_{diss}, μM phospholipid[b]	$[L]_{s,max}$, nmol of phospholipid/10^6 cells[b]	k_e, min^{-1}[c]
0	MMC-DSPE	81	12.1 ± 1.7[d]	4.26 ± 0.14	0.026
1.2	MMC-DSPE	71	38.3 ± 5.7	3.70 ± 0.16	0.033
3.5	MMC-DSPE	59	1211 ± 79	15.3 ± 0.8	0.014
5.7	MMC-DSPE	35	732 ± 11	10.5 ± 1.1	0.012
1.2[a]	MP-PEG (M_r 2000)-DSPE	89	13.1 ± 2.2	1.47 ± 0.05	0.026
3.5[a]	MP-PEG (M_r 2000)-DSPE	92	9.33 ± 3.93	1.09 ± 0.10	0.018
5.7[a]	MP-PEG (M_r 2000)-DSPE	124	8.62 ± 1.72	3.02 ± 0.13	0.023

[a] Total of methoxy-PEG-DSPE and maleimido-PEG-DSPE. [b] K_{diss} and $[L]_{s,max}$ were determined at 4 °C as described in the Materials and Methods section Immunoliposome Binding to Cells. [c] k_e was determined at 37 °C using the HPTS fluorescence method as described in Materials and Methods. [d] Mean ± SE.

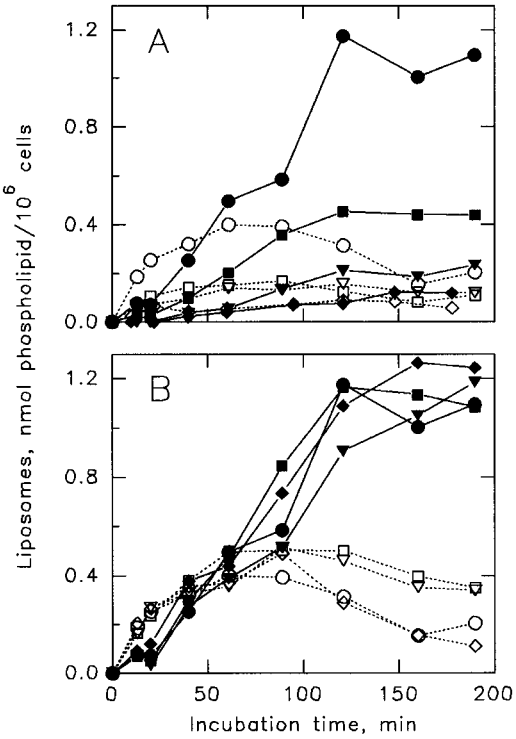

FIGURE 6: Effect of PEG-DSPE content on the uptake kinetics of anti-HER2 immunoliposomes by SK-BR-3 cells: (A) anti-HER2 Fab′ attached to the liposomes via a short spacer (MMC-DSPE); (B) Fab′ attached to PEG termini. Surface-bound liposomes: dashed line, hollow symbols. Endocytosed liposomes: solid line, filled symbols. PEG-DSPE content: none (○), 1.2 mol % (□), 3.5 mol % (▽), and 5.7 mol % (◇).

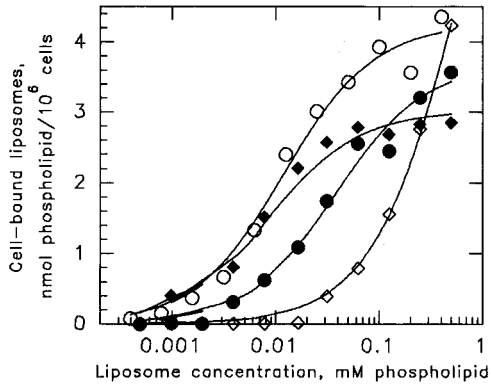

FIGURE 7: Binding of anti-HER2 immunoliposomes to SK-BR-3 cells at 4 °C. Fab′ attached via a short spacer (MMC-DSPE): no PEG-PE (○), 1.2 mol % PEG-DSPE (●), and 5.7 mol % PEG-DSPE (◇). Fab′ attached to PEG termini: 5.7 mol % PEG-DSPE (◆).

and even at 1.3 mol % of PEG-DSPE the reduction in cellular uptake was apparent (Figure 6A). On the contrary, anti-HER2-SL prepared with maleimido-PEG-DSPE as a linker showed no reduction in uptake even when the total liposome content of PEG-DSPE and maleimido-PEG-DSPE derivatives reached 5.7 mol % (Figure 6B).

Increasing PEG-DSPE content affected the cell surface binding affinity and k_e of anti-HER2-SL to HER2-overexpressing cells in a different way, dependent on whether the conjugation was *via* a short spacer or long (PEG) spacer. The binding curves (Figure 7) fit very well to the simple Langmuir-type equation of the equilibrium binding assuming all binding sites equal and independent (see eq 3 in Methods). As shown on Table 3, the presence of PEG on the liposome surface strongly affected the binding affinity of anti-HER2-SL prepared with the short linker (K_{diss} increased 60−100-fold when PEG-DSPE contents increased from 0 to 5.7 mol %) while the internalization rate of surface-bound liposomes was much less affected (k_e decreased only 2-fold). Again, surface-grafted PEG has practically no effect on the binding affinity or internalization rate of anti-HER2-SL prepared by conjugation of Fab′ fragments to the termini of PEG chains.

DISCUSSION

Attachment of anti-HER2 Fab′ to the distal termini of PEG chains on sterically stabilized immunoliposomes was explored as a means to avoid interference from the PEG chains with its interaction with the target, p185^{HER2}, on the cell surface. This approach has been successfully applied to enzymes (Blume *et al.*, 1993), small molecules (Lee & Low, 1994), and whole antibodies (Allen *et al.*, 1994, 1995; Hansen *et al.*, 1995; Maruyama *et al.*, 1995; Zalipsky et al., 1996). However, in the latter case, the increasing number of conjugated antibody molecules led to the increasing rate of immunoliposome clearance from the circulation, possibly because of the recognition of the Fc portion of conjugated antibody by macrophages. To avoid this problem, we have used Fab′ fragments as a targeting device (Martin & Papahadjopoulos, 1982; Park *et al.*, 1995). Additionally, the

thiol group in the hinge region provided a single site for conjugation far away from the antigen binding site, which also ensured correct orientation of the conjugated Fab′ (Nässander *et al.*, 1995; Shahinian & Silvius, 1996).

Two strategies for the synthesis of maleimide-terminated PEG-DSPE derivatives (Figure 1) yielded equally active products, but the use of a heterobifunctional PEG derivative was preferred since it allowed convenient one-step synthesis from commercially available precursors, DPPE and MP-PEG-SC. The stability of the maleimide function in the chosen groups (MP and MMC) at neutral pH proved to be sufficient to ensure quantitative conjugation of Fab′ fragments bearing reactive free thiols. When a short maleimide-terminated linker (MMC-PE) was used for Fab′ conjugation to the liposomes containing PEG-DSPE, the efficiency of conjugation somewhat decreased at PEG-DSPE concentrations corresponding to the predominantly brush conformation of the polymer (Figure 2), possibly due to the hindered penetration of the Fab′ fragment through the polymer "cloud"; however, the hindrance was less pronounced than expected from the theoretical prediction by Torchilin *et al.* (1994). This observation agrees with the results of Hansen *et al.* (1995), who found no decrease in the conjugation efficiency of the thiolated whole IgG to SL containing 5 mol % PEG-DSPE and activated with the short-chain maleimide linker (maleimidophenyl)butyryl-PE.

HER2-overexpressing cells showed considerable uptake of anti-HER2 SL, reaching 8000−23 000 vesicles/cell at saturating liposome concentrations. The selectivity of the uptake was also high: uptake by the cell line with low HER2 expression was at least 2 orders of magnitude lower than by HER2-overexpressing cells (Table 1). The same selectivity was achieved in the uptake of anti-HER2 immunoliposomes, with or without PEG-DSPE, by HER2-overexpressing cells (1−6 nmol/10^6 cells) in comparison to nontargeted SL ($\leq$0.01 nmol/10^6 cells). The quenching of excess active groups following the conjugation reaction seems to be important in achieving good selectivity of targeted liposome uptake, since in the presence of free thiols or hydrazide groups at the PEG termini, sterically stabilized immunoliposomes show appreciable background binding to the cells lacking the target antigen (Allen *et al.*, 1995; Hansen *et al.*, 1995), possibly due to nonspecific covalent attachment to cell surface molecules (thiol exchange or hydrazone formation with terminal sugar residues of cell surface glycoproteins).

Both confocal microscopy and spectrofluorometry of liposome-entrapped HPTS indicated endosomal localization of internalized anti-HER2 SL. Anti-HER2-SL bound to target cells became internalized and eventually, but not immediately, colocalized with endocytosed fluorescein-labeled transferrin (Figure 3). Since transferrin is shown to enter the cells by receptor-mediated endocytosis via a coated-pit mechanism and colocalize with the antibody-stimulated HER2 receptor (Maier *et al.*, 1991), this observation suggested that anti-HER2-SL are endocytosed through the similar process, likely associated with the internalization of the HER2 receptor. The internalization rate of anti-HER2-SL was visibly slower than that of transferrin, which was consistent with the kinetic data: k_e 0.018 min^{-1} for anti-HER2 SL (Table 3) vs 0.23 min^{-1} for the transferrin−receptor complex (Douglas & King, 1988). Since ^{125}I-labeled transferrin conjugated to liposomes of comparable size was shown to be internalized by transferrin receptor-bearing cells at the same rate as free ^{125}I-labeled transferrin (Vidal *et al.*, 1987), the difference in the endocytosis rates between transferrin and anti-HER2-SL is likely to reflect the difference in the endocytosis rates between the transferrin−receptor complex and the antibody-activated HER2 receptor.

The density of conjugated Fab′ on the liposome surface and the density of HER2 receptors on the cell surface were important determinants of the liposome uptake by the cells. The increasing density of Fab′ fragments on the liposome surface did not lead, however, to an unlimited increase in the cellular uptake, reaching a plateau at about 35−40 Fab′ per 100 nm liposome, or one antigen binding site per each 1000 phospholipid molecules in the outer leaflet of the liposome bilayer (Figure 5A). These results are in agreement with the observation that binding *in vivo* of SL conjugated via the PEG spacer to the antibody (34A) specific for murine lung endothelium reaches saturation at about 30 antibodies per 90−130 nm liposome, or about 1.2 binding sites per each 1000 phospholipid molecules of the outer leaflet (Maruyama *et al.*, 1995).

Comparison of the uptake of anti-HER2 immunoliposomes by cells with different levels of $p185^{HER2}$ expression showed that high expression of $p185^{HER2}$ was a necessary but evidently not sufficient condition for the high cellular uptake of anti-HER2 immunoliposomes (Table 1). The cellular uptake of anti-HER2 immunoliposomes best correlated with the antiproliferative activity of the murine prototype of the targeting antibody, 4D5 (Table 2). The antiproliferative effect of anti-HER2 MAb has been linked to its ability to cause receptor internalization (Tagliabue *et al.*, 1991; Sarup *et al.*, 1991). This observation suggested that the uptake of anti-HER2 immunoliposomes is determined not only by the density of HER2 protein but also by the ability to promote endocytosis of the HER2 receptor, which also implies that endocytosis of the anti-HER2 immunoliposome is a consequence of the endocytosis of its target antigen, $p185^{HER2}$. Since monovalent Fab′ fragments lack the agonistic and antiproliferative activity of the whole bivalent 4D5 antibody (Sarup *et al.*, 1991), it further implies that immunoliposomes bearing conjugated anti-$p185^{HER2}$ Fab′ fragments act as multivalent immunoligands capable of receptor stimulation similar to the bivalent antibody. Indeed, after a few hours of incubation with SKBR-3 cells about 50% of cell-associated immunoliposomes bearing as few as 6 anti-HER2 Fab′ fragments per vesicle were endocytosed, and cell-associated immunoliposomes bearing at least than 15 Fab′/vesicle were endocytosed with more than 80% efficiency (Figure 5B).

The attachment of targeting antibody to the termini of surface-grafted PEG chains, rather than in close proximity of the liposome bilayer, has been shown to improve the association of immunoliposomes with their target cells (Hansen *et al.*, 1995). However, in these studies the processes of surface binding and subsequent internalization of PEG-derivatized immunoliposomes were not discriminated, and the separate effects of surface-grafted PEG on these two processes still remained to be clarified. The use of the HPTS method (Straubinger *et al.*, 1990) allowed simultaneous quantitation of immunoliposome binding and endocytosis by HER2-overexpressing cells and provided evidence that decreased surface binding affinity is the major reason for the reduced cellular uptake of anti-HER2-SL with targeting Fab′ fragments attached proximally to the liposome bilayer. While the efficiency of endocytosis of surface-bound

anti-HER2 immunoliposomes, measured as the first-order internalization rate constant (k_i), decreased only 2-fold when the PEG-DSPE content increased from 0% to 5.7 mol %, the binding affinity of immunoliposomes decreased by almost 2 orders of magnitude (Table 3). Uptake of anti-HER2 immunoliposomes incubated with SK-BR-3 cells at a concentration (25 μM) close to K_{diss} (12 μM) reached the plateau at a Fab′ density of more than 35−40 Fab′/liposome (Figure 5); therefore, such dramatic reduction in affinity could not be explained by the lower coupling efficiency of high-PEG vs low-PEG liposomes (35 Fab′/liposome vs 81 Fab′/liposome), and in accordance with the results obtained in similar systems (Kibanov *et al.*, 1990; Torchilin *et al*., 1995), it was attributed to the effect of surface-grafted PEG. The extension length of the grafted PEG in the brush conformation on the surface of phosphatidylcholine liposomes containing 6 mol % PEG (M_r 2000)-DSPE is approximately 6 nm (Kenworthy *et al.*, 1995a,b) while the length of the Fab′ molecule has been determined as 7 nm from X-ray crystallography data (Nezlin, 1977). Apparently, the repulsion between cell surface and liposome PEG coating decreases the free energy gain of the Fab′ binding to p185^{HER2} on the cell surface, therefore reducing the apparent affinity constant ($\Delta G^\circ = -RT \ln K$). When the antigen binding site was located outside of the PEG coat, e.g., in the case of the Fab′ attachment to the distal termini of PEG chains, cell surface binding of immunoliposomes was not affected by PEG (Table 2).

Cell surface binding parameters of anti-HER2 immunoliposomes with fully exposed antigen binding sites, i.e., prepared in the absence of PEG-DSPE or by terminal conjugation of Fab′ to PEG chains, were in good agreement with the cell binding parameters of the muMAb 4D5, a prototype of the targeting antibody rhuMAbHER2. To allow comparison, K_{diss} (Table 3) was translated from the units of liposomal phospholipid concentration to the molar concentration units of conjugated anti-HER2 Fab′. The resulting values and maximum numbers of binding sites per cell were 9−12 nM and (0.7−4.4) $\times$ 10^6, respectively, compared to 19 nM and 2 $\times$ 10^6 for free 4D5 Fab and 6 nM and 0.93 $\times$ 10^6 for free 4D5 MAb (Sarup *et al.*, 1991). Immunoliposomes with high PEG-DSPE content and lower binding affinity to the cells tended to saturate the cellular uptake mechanism at higher levels. We may hypothesize that PEG coating reduces the lateral mobility of the liposome-conjugated Fab′ fragment and therefore reduces the number of Fab′ fragments that can become exposed at the contact surface between the liposome and the cell membrane, so that each immunoliposome endocytosis event consumes less molecules of the target antigen. However, it is likely that, for *in vivo* applications, the saturation binding will be less important than affinity, since the concentrations of targeted liposomes in the body tissues are unlikely to come close to saturation values.

Antibody binding to the cell surface proteins of the EGFR family often induces their internalization. It was of interest to compare the rates of immunoliposome internalization (k_e 0.012−0.033 min^{-1}; Table 3) with the rates of antibody-induced internalization of their target antigen. Since the endocytic rate constants for rhuMAbHER2-activated p185^{HER2} were unavailable, the comparison was made with Neu protein, a rat homolog of human p185^{HER2}. Using the data of Gilboa *et al*. (1995), we have estimated that the wild-type Neu activated by a bivalent agonistic antibody, as well as Neu*, a constitutively dimerized, permanently activated point mutant of Neu, expressed in NIH 3T3 cells, was endocytosed with k_e 0.024 min^{-1}, while Neu bound to nonagonistic Fab fragments of the same antibody had k_e 0.013 min^{-1}. The latter value is practically equal to that observed by us for anti-HER2 SL coated with PEG in brush conformation and bearing anti-HER2 Fab′ attached through a short spacer (Table 3, ≥3.5 mol % PEG-DSPE). Such twofold decrease in k_e, compared to that of liposomes with fully exposed Fab′, may be caused by PEG chains creating repulsion between HER2 molecules held by the liposome-attached Fab′, therefore preventing HER2 dimerization necessary to promote endocytosis. Comparison of the kinetic data, together with the confocal microscopy data and the strong correlation between immunoliposome uptake and agonistic action of the targeting antibody, leads us to conclude that the endocytosis of anti-HER2 immunoliposomes is strongly associated with the endocytosis of their target antigen, p185^{HER2}. Binding of immunoliposomes to their target cells is not always followed by the liposome internalization (Leserman & Machy, 1987). Goren et al. (1996) found that anti-HER2-SL constructed using a different targeting antibody (N-12A5), as well as a different conjugation method, selectively bind to HER2-positive human gastric carcinoma cancer cells (N-87) but do not increase the drug cytotoxicity *in vitro*, or its antitumor effect *in vivo*, compared to nontargeted doxorubicin-loaded SL, probably due to lack of cell internalization. Therefore, appropriate choice of the targeting antibody, as well as of the target antigen, may be crucial for successful development of pharmaceutical immunoliposomes capable of intracellular drug delivery.

We have described sterically stabilized immunoliposomes which efficiently bind to the cancer cells overexpressing p185^{HER2} oncoprotein and enter cells through endocytosis. The specificity of binding was achieved by conjugation of a Fab′ fragment of the recombinant humanized antibody against extracellular domain of HER2, while steric stabilization of the liposomes was provided by an amphiphilic poly(ethylene glycol) derivative PEG-DSPE. To prevent PEG chains from interferring with the antibody−antigen interaction, the target-specific antibody fragments were conjugated to the distal termini of liposome-grafted PEG chains modified with maleimide groups; free thiol groups in the area of Fab′ corresponding to the antibody hinge region were used for conjugation. The resulting sterically stabilized immunoliposomes showed unperturbed binding and internalization by HER2 overexpressing cancer cells in cell culture even at high PEG-DSPE content.

Recent advances in liposome research, including development of sterically stabilized liposomes, increased attention to liposomes as delivery vehicles for cancer treatment drugs (Lasic & Papahadjopoulos, 1995). Among the advantages offered by sterically stabilized drug-loaded liposomes are improved plasma pharmacokinetics, higher storage stability, higher tumor localization of the drug, and improved therapeutic index (Papahadjopoulos *et al.*, 1991; Gabizon, 1992; Lasic & Martin, 1995). Anticancer drugs such as doxorubicin can be stably and efficiently loaded into sterically stabilized anti-HER2 immunoliposomes as well (Park *et al.*, 1995). Preliminary results indicated that the described design of anti-HER2-SL results in the decreased blood clearance similar to that of unmodified SL and to higher efficacy of such HER2-targeted cytostatic SL, compared to their nontargeted counterparts, for the growth inhibition of HER2-

overexpressing breast cancer xenografts in nude mice (Park *et al.*, 1996). Targeting directed by an anti-p185^{HER2} antibody which endows sterically stabilized liposomes with the capability of carrying their drug load inside the target cancer cell will add a new dimension to the technology of liposomal drug delivery.

REFERENCES

Allen, T. M., Agrawal, A. K., Ahmad, I., Hansen, C. B., & Zalipsky, S. (1994) *J. Liposome Res. 4*, 1−25.

Allen, T. M., Brandeis, E., Hansen, C. B., Kao, G. Y., & Zalipsky, S. (1995) *Biochim. Biophys. Acta 1237*, 99−108.

Bator, J. M., & Reading, C. L. (1991) in *Therapeutic Monoclonal Antibodies* (Borrebaeck, C. A. K., & Larride, J. W., Eds.) pp 35−56, M. Stockton Press, New York.

Begent, R. H. J. (1990) in *Genes and Cancer* (Carney, D., & Sikora, K., Eds.) pp 173−183, Wiley, Chichester.

Blume, G., Cevc, G., Crommelin, M. D. J. A., Baker-Woudenberg, I. A. J. M., Kluft, C., & Storm, G. (1993) *Biochim. Biophys. Acta 1149*, 180−184.

Bradford, M. (1976) *Anal. Biochem. 72*, 248−254.

Carter, P., Presta, L., Gorman, C. M., Ridgway, J. B. B., Henner, D., Wong, W. L. T., Rowland, A. M., Kotts, C., Carver, M. E., & Shepard, H. M. (1992) *Proc. Natl. Acad. Sci. U.S.A. 89*, 4285−4289.

De Potter, C. R. (1994) *Hum. Pathol. 25*, 1264−1268.

Douglas, G. C., & King, B. F. (1988) *Placenta 9*, 253−265.

Eccles, S. A., Court, W. J., Box, G. A., Dean, C. J., Melton, R. G., & Springer, C. J. (1994) *Cancer Res. 54*, 5171−5177.

Emanuel, N., Kedar, E., Bolotin, E. M., Smorodinsky, N. I., & Barenholz, Y. (1996) *Pharmacol. Res. 13*, 352−359.

Fominaya, J., & Wels, W. (1996) *J. Biol. Chem. 27*, 10560−10568.

Gabizon, A. (1992) *Cancer Res. 52*, 891−896.

Gilboa, L., Ben-Levy, R., Yarden, Y., & Henis, Y. I. (1995) *J. Biol. Chem. 270*, 7061−7067.

Goren, D., Horowitz, A. T., Zalipsky, S., Woodle, M. C., Yarden, Y., & Gabizon, A. (1996) *Br. J. Cancer* (in press).

Hansen, C. B., Kao, G. Y., Moase, E. H., Zalipsky, S., & Allen, T. M. (1995) *Biochim. Biophys. Acta 1239*, 133−144.

Hudziak, R. M., Lewis, G. D., Winget, M., Fendly, B. M., Shepard, H. M., & Ullrich, A. (1989) *Mol. Cell. Biol. 9*, 1165−1172.

Kenworthy, A. K., Simon, S. A., & McIntosh, T. J. (1995a) *Biophys. J. 68*, 1903−1920.

Kenworthy, A. K., Hristova, K., Needham, D., & McIntosh, T. J. (1995b) *Biophys. J. 68*, 1921−1936.

King, S. E., & Schottenfeld, D. (1996) *Oncology 53*, 453−462.

Klibanov, A. L., Maruyama, K., Beckerleg, A. M., Torchilin, V. P., & Huang, L. (1990) *Biochim. Biophys. Acta 1062*, 142−148.

Lasic, D., & Martin, F., Eds. (1995) *Stealth Liposomes*, 289 pp, CRC Press, Boca Raton, FL.

Lasic, D., & Papahadjopoulos, D. (1995) *Science 267*, 1275−1276.

Lee, K.-D., Nir, S., & Papahadjopoulos, D. (1993) *Biochemistry 32*, 889−899.

Lee, R. J., & Low, P. S. (1994) *J. Biol. Chem. 269*, 3198−3204.

Leserman, L., & Machy, P. (1987) in *Liposomes: From Biophysics to Therapeutics* (Ostro, M. J., Ed.) pp 157−194, Marcel Dekker, New York.

Lewis, G. D., Figari, I., Fendly, B., Wong, W.-L., Carter, P., Gorman, C., & Shepard, H. M. (1993) *Cancer Immunol. Immunother. 37*, 255−263.

Maier, L. A., Xu, F. J., Hester, S., Boyer, C. M., McKenzie, S., Bruskin, A. M., Argon, Y., & Bast, R. C., Jr. (1991) *Cancer Res. 51*, 5361−5369.

Marsh, D. A. (1990) *CRC Handbok of Lipid Bilayers*, pp 163−168, CRC Press, Boca Raton, FL.

Martin, F., & Papahadjopoulos, D. (1982) *J. Biol. Chem. 257*, 286−288.

Maruyama, K., Takizawa, T., Yuda, T., Kennel, S. J., Huang, L., & Iwatsuru, M. (1995) *Biochim. Biophys. Acta 1234*, 74−80.

Molland, J. G., Barraclough, B. H., Gebski, V., Milliken, J., & Bilous, M. (1996) *Aust. N.Z. J. Surg. 66*, 64−70.

Morrison, W. R. (1964) *Anal. Biochem. 7*, 281−224.

Nässander, U. K., Steerenberg, P. A., De Jong, W. H., Van Overveld, W. O. W. M., Te Boekhorst, C. M. E., Poels, L. G., Jap, P. H. K., & Storm, G. (1995) *Biochim. Biophys. Acta 1235*, 126−139.

Nezlin, R. C. (1977) *Structure and Biosynthesis of Antibodies*, p 174, Consultants Bureau, New York.

Olson, F., Hunt, C. A., Szoka, F. C., Vail, W. J., & Papahadjopoulos, D. (1979) *Biochim. Biophys. Acta 557*, 9−23.

Papahadjopoulos, D., & Gabizon, A. A. (1995) in *Liposomes as Tools in Basic Research and Industry* (Philippot, J. R., & Schuber, F., Eds.) pp 177−188, CRC Press, Boca Raton, FL.

Papahadjopoulos, D., Allen, T. M., Gabizon, A., Mayhew, E., Matthay, K., Huang, S.K., Lee, K.-D., Woodle, M. C., Lasic, D. D., & Redemann, C. (1991) *Proc. Natl. Acad. Sci. U.S.A. 88*, 11640−11464.

Park, J. W., Stagg, R., Lewis, G. D., Carter, P., Maneval, D., Slamon, D. J., Jaffe, H., & Shepard, H. M. (1992) in *Genes, Oncogenes, and Hormones: Advances in Cellular and Molecular Biology of Breast Cancer* (Dickson, R. B., & Lippman, M. E., Eds.) pp 193−211, Kluwer, Boston.

Park, J. W., Hong, K., Carter, P., Asgari, H., Guo, L. Y., Keller, G. A., Wirth, C., Shalaby, R., Kotts, C., Wood, W. I., Papahadjopoulos, D., & Benz, C. C. (1995) *Proc. Natl. Acad. Sci. U.S.A. 92*, 1327−1331.

Park, J. W., Colbern, G., Baselga, J., Hong, K., Shao, Y., Kirpotin, D., Nuigens, A., Wood, W., Papahadjopoulos, D., & Benz, C. C. (1996) *Proc. ASCO 15*, 501.

Press, M. F., Cordon-Cardo, C., & Slamon, D. J. (1990) *Oncogene 5*, 953−962.

Rodrigues, M. L., Presta, L. G., Kotts, C. E., Wirth, C., Mordenti, J., Osaka, G., Wong, W. L., Nuijens, A., Blackburn, B., Carter, P. (1995) *Cancer Res. 55*, 63−70.

Rodriguez, G. C., Boente, M. P., Berchuck, A., Whitaker, R. S., O'Briant, K. C., Xu, F., & Bast, R. C., Jr. (1993) *Am. J. Obstet. Gynecol. 168*, 228−232.

Sarup, J. C., Johnson, R. M., King, K. L., Fendly, B. M., Lipari, M. T., Napier, M. A., Ullrich, A., & Shepard, H. M. (1991) *Growth Regul. 37*, 72−82.

Scott, G. K., Robles, R., Park, J. W., Montgomery, P. A., Daniel, J., Holmes, W. E., Lee, J., Keller, G. A., Li, W.-L., Fendly, B. M., Wood, W. I., Shepard, H. M., & Benz, C. C. (1993) *Mol. Cell. Biol. 13*, 2247−2257.

Sedlack, J., & Lindsay, R. H. (1968) *Anal. Biochem. 25*, 192−205.

Shahinian, S., & Silvius, J. R. (1995) *Biochim. Biophys. Acta 1239*, 157−167.

Shalaby, M. R., Carter, P., Maneval, D., Giltinan, D., Kotts, C. (1995) *Clin. Immunol. Immunopathol. 74*, 185−192.

Slamon, D. J., Godolphin, W., Jones, L. A., Holt, J. A., Wong, S. G., Keith, D. E., Levin, W. I., Stuart, S. G., Udove, J., Ullrich, A., & Press, M. (1989) *Science 244*, 707−712.

Straubinger, R. M., Papahadjopoulos, D., & Hong, K. (1990) *Biochemistry 29*, 4929−4939.

Tagliabue, E., Centis, P., Campiglio, M., Mastroiannini, A., Martignone, S., Pellegrini, R., Casalani, P., Lanzi, C., Menard, S., & Colnaghi, M. I. (1991) *Int. J. Cancer 47*, 933−937.

Torchilin, V. P., Omelyanenko, V. G., Papisov, M. I., Bogdanov, A. A., Trubetskoy, V.S., Herron, J. N., & Gentry, C. A. (1994) *Biochim. Biophys. Acta 1995*, 11−20.

Tripathy, D., & Benz, C. C. (1992) *Cancer Treat. Res. 63*, 15−60.

Vidal, M., Sainte-Marie, J., Philippot, J. R., & Bienvenue, A. (1987) *FEBS Lett. 216*, 159−163.

Wels, W., Moritz, D., Schmidt, M., Jeschke, M., Hynes, N. E., & Groner, B. (1995) *Gene 159*, 73−80.

Woodle, M. C., & Lasic, D. D. (1992) *Biochim. Biophys. Acta 1113*, 171−199.

Zalipsky, S. (1993) *Bioconjugate Chem. 4*, 296−299.

Zalipsky, S., Brandeis, E., Newman, M., & Woodle, M. C. (1994) *FEBS Lett. 353*, 71−74.

Zalipsky, S., Hansen, C. B., Lopes de Menezes, D. E., & Allen, T. M. (1996) *J. Controlled Release 39*, 153−161.

Zhu, Z., Lewis, G. D., & Carter, P. (1995) *Int. J. Cancer 62*, 319−324.

BI962148U